

## Supplementary Information for “Theoretical Analysis of a Magnetophoresis-Diffusion T-Sensor Immunoassay”

Thomas P. Forbes,<sup>a</sup> Matthew S. Munson<sup>b</sup> and Samuel P. Forry<sup>b</sup>

<sup>a</sup> Materials Measurement Science Division, National Institute of Standards and Technology, Gaithersburg, MD, USA; <sup>b</sup> Biosystems and Biomaterials Division, National Institute of Standards and Technology, Gaithersburg, MD, USA

### Derivation of the Precision Profiles

Here, we present additional details and further development of the precision profile derivation found in the article text.

Four-parameter logistic curve:

$$\text{response} = D + \frac{(A-D)}{(1+(\text{dose}/C)^B)} \quad \text{or} \quad y = D + \frac{(A-D)}{(1+(x/C)^B)} \quad (\text{S1})$$

where,  $A$  is the response at zero dose and experimentally represents the nonspecific binding,  $B$  is the effective slope,  $C$  is the dose expected to give a response 50 % of the maximum achievable, and  $D$  is the response for infinite dose (maximum response). The response and dose will be referred to as “ $y$ ” and “ $x$ ” respectively.

Two parameter exponential relationship:  $\sigma^2(y) = \beta y^\theta$  (S2)

where,  $y$  is the raw response from Equation (S1),  $\sigma^2(y)$  is the variance of the response, and  $\beta$  and  $\theta$  are the parameters.<sup>1-3</sup> In order to determine the limit of detection and the dynamic range, we first created the precision profiles based on the relative standard deviation of the dose ( $\text{RSD}_{\text{dose}}$ ). With the use of the dose-response curve (Equation (S1)) fitted to the experimental and the response-error relationship (Equation (S2)), the theoretical relative standard deviation of the dose ( $\text{RSD}_{\text{dose}}$ ) was derived from the RSD of the response ( $\text{RSD}_{\text{resp}}$ ).<sup>3-5</sup> This was done for each dose by first converting the RSD of the response (Equation (S3)), normalized fluorescence intensity, to the standard deviation of the response ( $\text{SD}_{\text{resp}}$ , Equation (S4)) using Equations (S1) and (S2).

$$\text{RSD}_{\text{resp}} = \sqrt{\frac{\sigma^2(y)}{y^2}} \quad (\text{S3})$$

$$\text{SD}_{\text{resp}} = \text{RSD}_{\text{resp}} y = \sqrt{\beta y^\theta} = \sqrt{\beta \left[ D + \frac{(A-D)}{(1+(x/C)^B)} \right]^\theta} \quad (\text{S4})$$

Next, the SD of the response was converted to the SD of the dose ( $SD_{\text{dose}}$ ) by dividing by the slope of the dose-response, or calibration curve.

$$SD_{\text{dose}} = \frac{SD_{\text{resp}}}{(dy/dx)} = \frac{SD_{\text{resp}}}{\left[ \frac{(A-D)(x/C)^{B-1}B}{(C+(1+(x/C)^B)^2)} \right]} \quad (\text{S5})$$

Finally, the RSD of the dose was calculated by dividing the SD of the dose by the dose or sample antigen concentration.

$$RSD_{\text{dose}} = SD_{\text{dose}}/x \quad (\text{S6})$$

With the  $RSD_{\text{dose}}$  for each sample antigen concentration considered, the precision profile, can be created. The limit of detection and dynamic range are determined directly for the precision profile for a given system. Detailed discussion of this process can be found in the literature.<sup>2-5</sup>

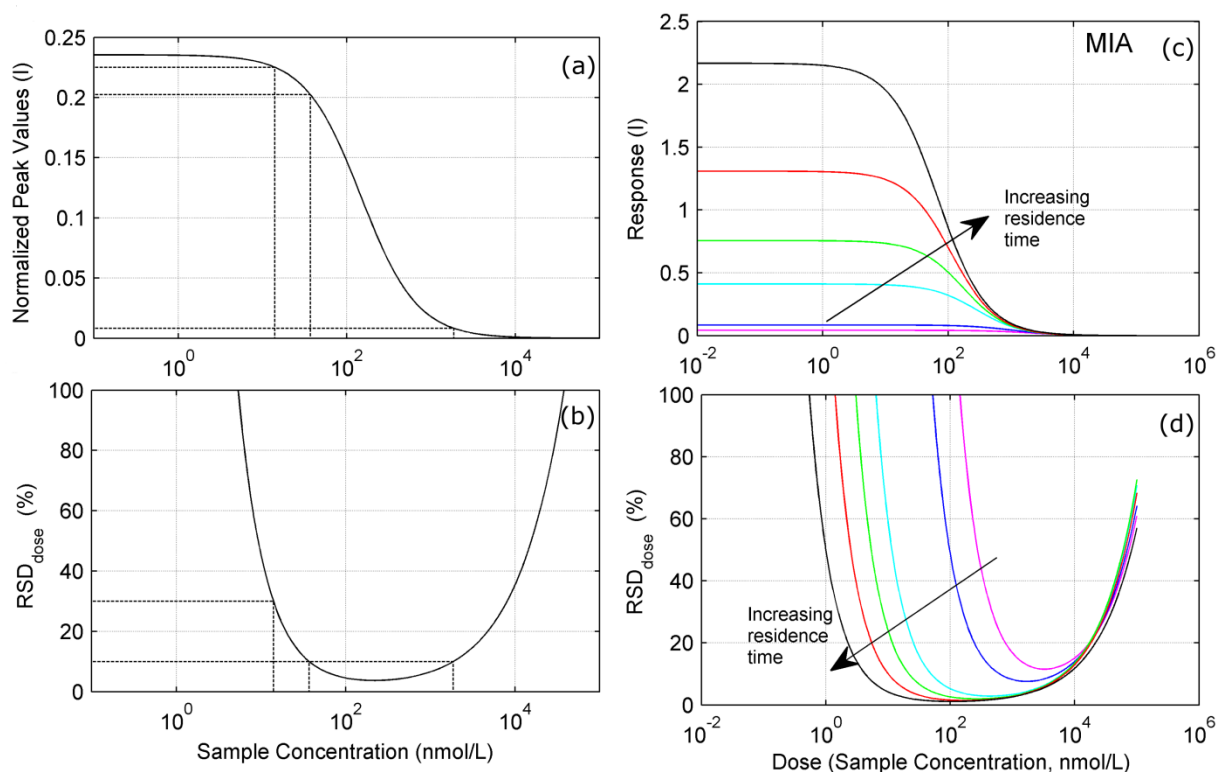


**Figure S1.** Examples of the limit of detection ( $RSD = 30\%$ ) and dynamic range ( $RSD < 10\%$ ) displayed on (a) the dose-response curve and (b) precision profile. (c) MIA dose-response curves and (d) precision profiles ( $RSD$  versus dose) as a function of increasing residence time for 10 nm superparamagnetic nanoparticles with 10  $\mu\text{m/s}$  magnetophoretic velocity. Residence times of 0.5, 1, 5, 10, 20, and 45 seconds are displayed. Examples of the limit of detection ( $RSD = 30\%$ ) and dynamic range ( $RSD < 10\%$ ) displayed on (a) the dose-response curve and (b) precision profile.

### ***Antigen and Antibody Site Concentrations***

We provide a brief discussion on the effect that the labeled antigen and antibody concentrations had on the diffusion immunoassay (DIA) response (or concentration of antibody sites in the case of nanoparticles, NP-DIA and MIA). Concentrations of the analyte are determined by the application, but the concentrations of the labeled antigen and antibody can be varied to provide optimal performance to be used for the remaining investigations. Figure S2 demonstrates the limit of detection as a function of the ratio of antibody concentration (or antibody site concentration) to labeled antigen concentration for three cases. As a starting point, the range of concentrations chosen were centered around relevant concentrations for therapeutic drugs, such as phenytoin,<sup>6</sup> in blood. The limit of detection was determined as defined above for varying the antibody concentration from 5 nmol/L to 1500 nmol/L, holding the labeled antigen constant at 5 nmol/L (-■-) and 50 nmol/L (-◆-), and for varying the labeled antigen concentration from 0.05 nmol/L to 1000 nmol/L, holding the antibody constant at 150 nmol/L (-●-). When the labeled antigen concentration was held constant, at large  $C_{Ab}/C_{A^*}$  ratios, the large number of binding sites required significant sample antigen concentrations for the competitive reactions to induce a change in the fluorescence distribution, resulting in high (poor) limits of detection. In contrast, for low  $C_{Ab}/C_{A^*}$  ratios, the antibody sites are saturated with labeled antigen and yet again required high levels of sample antigen for a distinguishable signal. When the concentration of antibody sites was held constant, at low  $C_{Ab}/C_{A^*}$  ratios the antibody sites are again saturated with labeled antigen leading to poor limits of detection. However, as the ratio increases, the limit of detection decreases to a constant value (Figure S2). This behavior can be attributed to the method of signal quantification, specifically, that each fluorescence distribution was normalized by the distribution of freely diffusing (zero reaction rate) labeled antigen. Therefore, even for very low concentrations of labeled antigen, the signal was normalized by this value. Based on the results in Figure S2, we identified the optimal antibody and labeled antigen concentrations to be 150 nmol/L and between 5 nmol/L to 50 nmol/L, respectively.

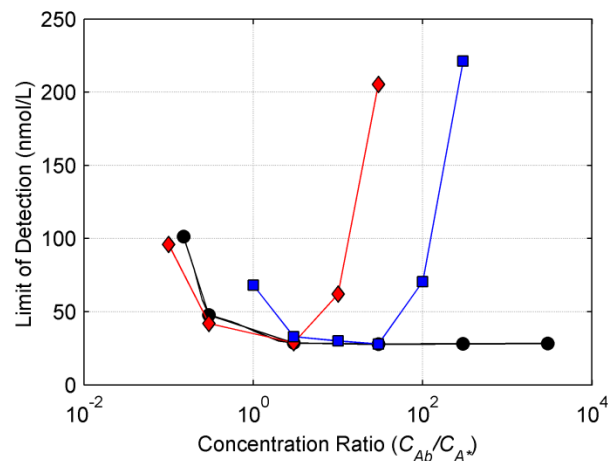


**Figure S2.** (Color online) DIA limit of detection as a function of antibody and labeled antigen concentrations: (-♦-)  $C_{Ab} = 5$  nmol/L to 1500 nmol/L and  $C_{A^*} = 50$  nmol/L (constant), (-■-)  $C_{Ab} = 5$  nmol/L to 1500 nmol/L and  $C_{A^*} = 5$  nmol/L (constant), (-●-)  $C_{Ab} = 150$  nmol/L (constant) and  $C_{A^*} = 0.05$  nmol/L to 1000 nmol/L.

### Dimensional Data

Additional dimensional plots of data referenced in the text are displayed here.

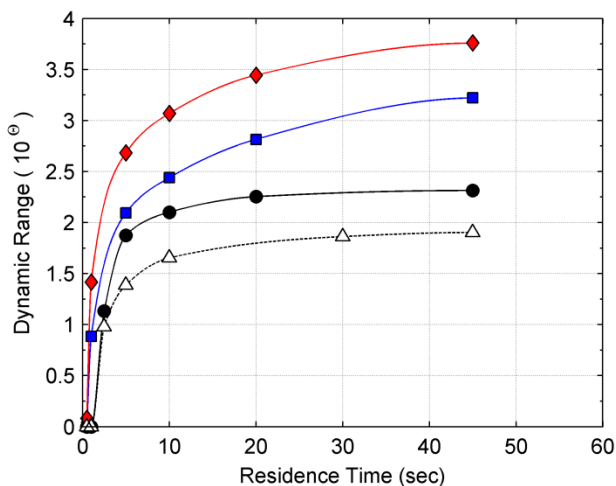


**Figure S3.** Dynamic range as a function of residence time (distance to detection point) for (-△-) DIA with 10 nm antibodies, (-●-) NP-DIA with 50 nm antibody-conjugated nanoparticles, (-■-) MIA with 10 nm superparamagnetic nanoparticles and 10  $\mu$ m/s magnetophoretic velocity, and (-♦-) MIA with 10 nm superparamagnetic nanoparticles and 50  $\mu$ m/s magnetophoretic velocity.

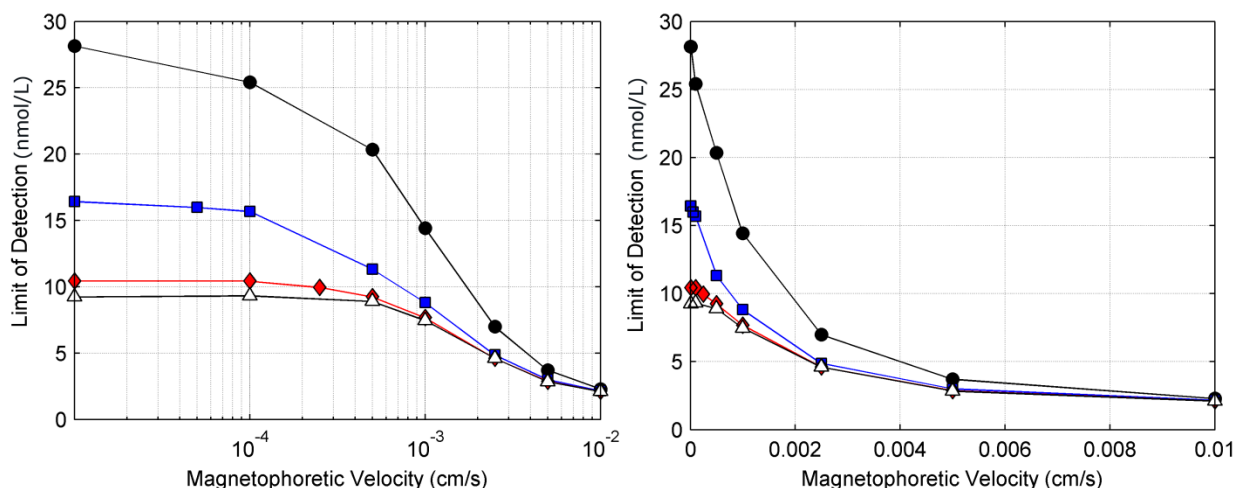


**Figure S4.** MIA limit of detection as a function of magnetophoretic velocity for (- $\Delta$ -) 250 nm, (- $\blacklozenge$ -) 150 nm, (- $\blacksquare$ -) 50 nm, and (- $\bullet$ -) 10 nm superparamagnetic antibody-coated nanoparticles.

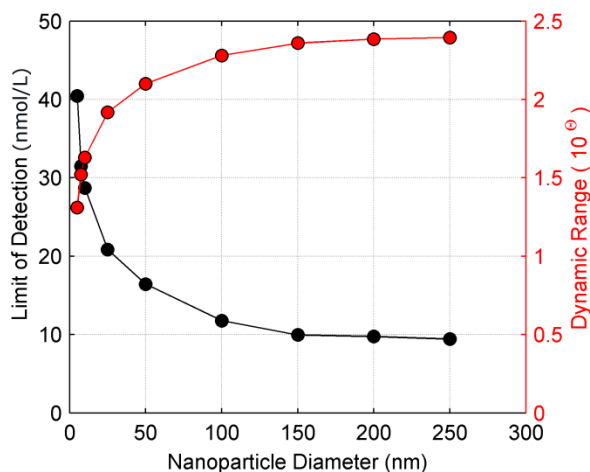


**Figure S5.** NP-DIA limit of detection (left ordinate axis) and dynamic range (right ordinate axis) as a function of nanoparticle diameter for a diffusion immunoassay.

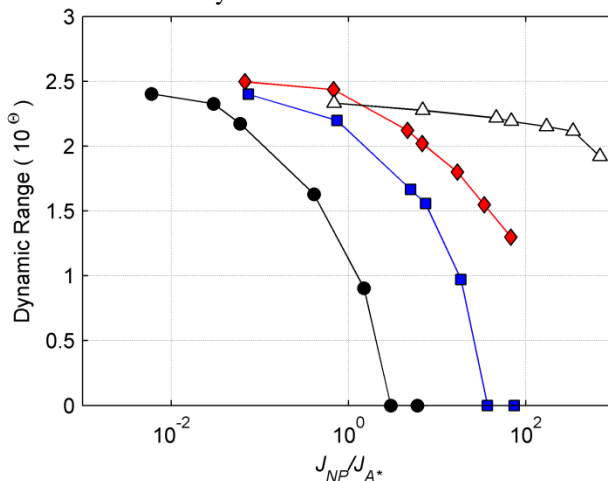


**Figure S6.** Dynamic range as a function of antigen diameter for diffusion and a couple superparamagnetic nanoparticle sizes, (- $\bullet$ -) antibody/nanoparticle diffusion, (- $\blacksquare$ -) 10 nm nanoparticle at 1  $\mu\text{m/s}$ , (- $\blacklozenge$ -) 50 nm nanoparticle at 1  $\mu\text{m/s}$ , and (- $\Delta$ -) 10 nm nanoparticle at 10  $\mu\text{m/s}$  magnetophoretic velocity.

## Dose-Response Curves and Precision Profiles

Additional calibration (dose-response) curves and precision profiles for a number of variables.

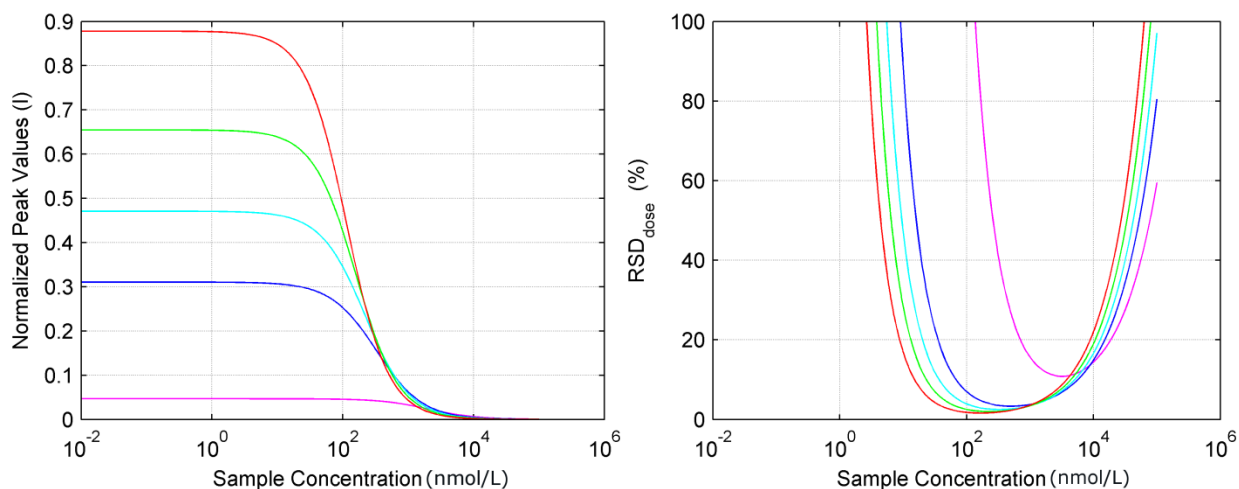


**Figure S7.** (a) NP-DIA dose-response curves and (b) precision profiles (RSD versus concentration) as a function of increasing residence time for a purely diffusion immunoassay with 50 nm antibody-conjugated nanoparticles. Residence times of 0.5, 5, 10, 20, and 45 seconds are displayed.

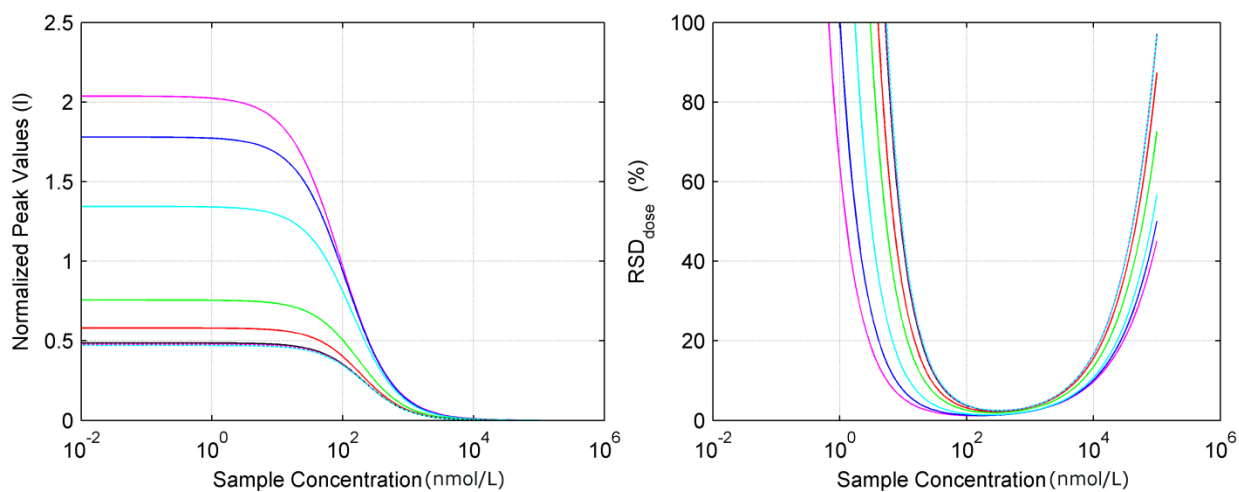


**Figure S8.** (a) MIA dose-response curves and (b) precision profiles as a function of increasing magnetophoretic velocity for 50 nm superparamagnetic nanoparticles. Magnetophoretic velocities range from 0.1 nm/s to 100  $\mu$ m/s.

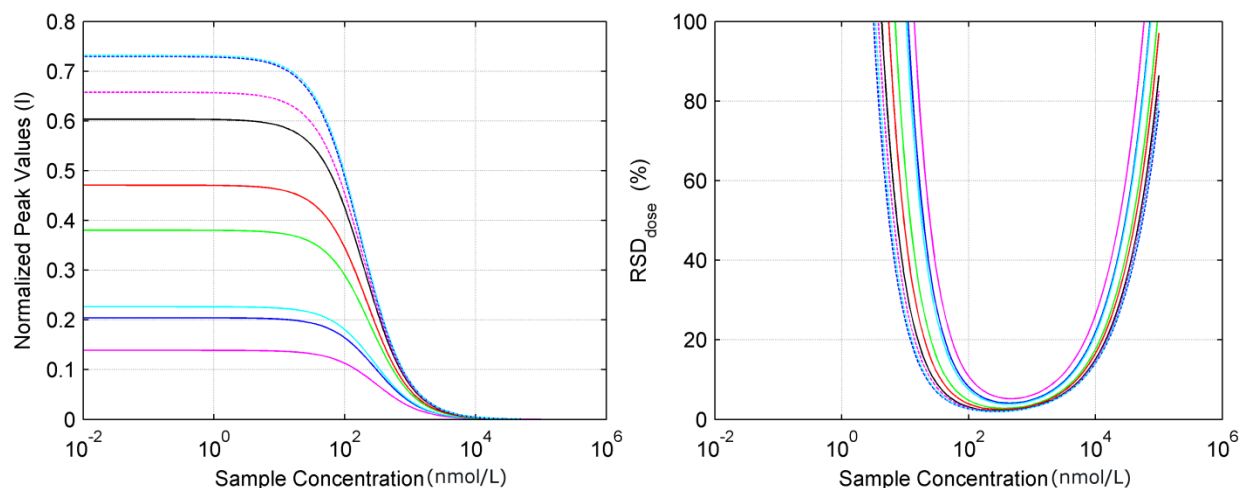


**Figure S9.** (a) NP-DIA dose-response curves and (b) precision profiles (RSD versus concentration) as a function of nanoparticle diameter for a purely diffusion immunoassay. Nanoparticle diameters range from 5 nm to 250 nm.

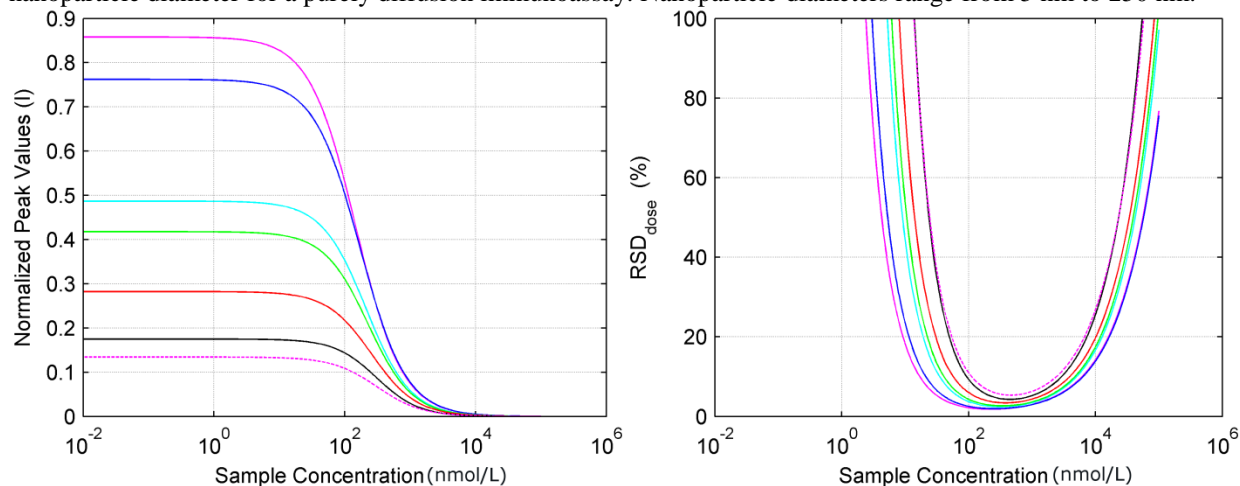


**Figure S10.** (a) MIA dose-response curves and (b) precision profiles as a function of antigen size for 50 nm superparamagnetic nanoparticles with 1  $\mu\text{m/s}$  magnetophoretic velocity. Antigen diameters range from 0.01 nm to 10 nm.

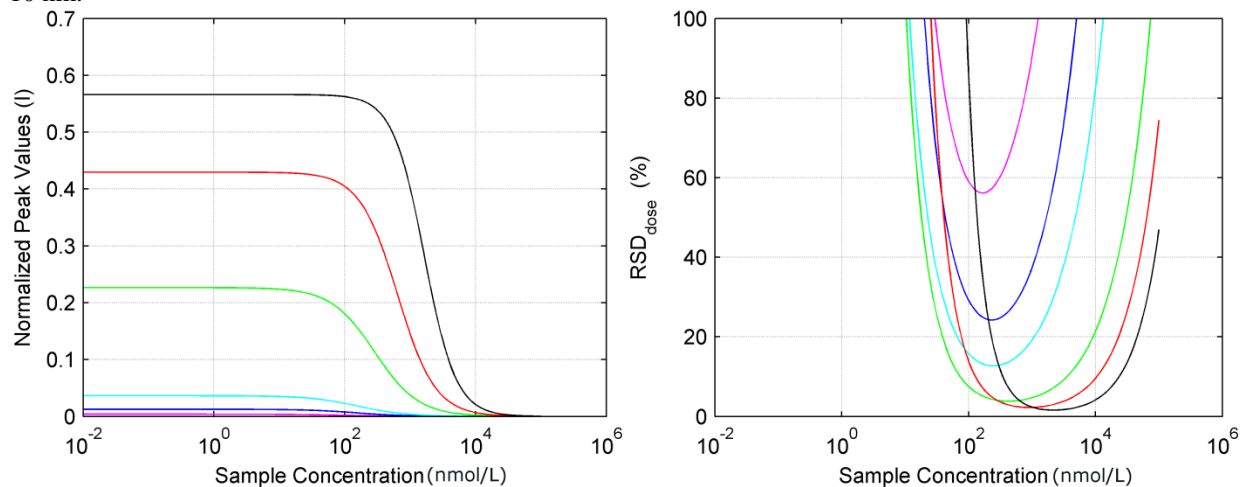


**Figure S11.** (a) DIA dose-response curves and (b) precision profiles (RSD versus concentration) as a function of antibody site concentration with 50 nmol/L labeled antigen concentration for a diffusion immunoassay. Antibody site concentrations range from 1.5 nmol/L to 1.5  $\mu\text{mol/L}$ .

## References

1. G.M. Raab, *Journal of the Royal Statistical Society. Series C (Applied Statistics)*, 1981, **30**, 32-40.
2. W.A. Sadler and M.H. Smith, *Clinical Chemistry*, 1985, **31**, 1802-1805.
3. W.A. Sadler, M.H. Smith and H.M. Legge, *Clinical Chemistry*, 1988, **34**, 1058-1061.
4. R.A. Dudley, P. Edwards, R.P. Ekins, D.J. Finney, I.G. McKenzie, G.M. Raab, D. Rodbard and R.P. Rodgers, *Clinical Chemistry*, 1985, **31**, 1264-1271.
5. Y. Hayashi, R. Matsuda, T. Maitani, K. Imai, W. Nishimura, K. Ito and M. Maeda, *Analytical Chemistry*, 2004, **76**, 1295-1301.
6. A. Hatch, A.E. Kamholz, K.R. Hawkins, M.S. Munson, E.A. Schilling, B.H. Weigl and P. Yager, *Nat Biotech*, 2001, **19**, 461-465.